APPLICATION OF REMOTE SENSING IN LITHOLOGICAL DISCRIMINATION AND GEOLOGICAL MAPPING OF PRECAMBRIAN BASEMENT ROCKS IN THE EASTERN DESERT OF EGYPT

Mohamed F. Sadek and Safaa M. Hasan

National Authority for Remote Sensing and Space Sciences (NARSS), Cairo, Egypt.

E-mail: mfsadek@gmail.com

KEY WOEDS: Egypt; Basement rocks; Gabal Gharib; Gabal Gerf; ETM ratio image; Egyptsat-1; Data fusion.

Abstract: The late Proterozoic Precambrian basement rocks exposed at the extreme northern part of the Eastern Desert of Egypt comprising metavolcanics, Dokhan volcanics intruded by syn-to late-to post magmatic granitic intrusions. They are unconformably overlain by Quaternary deposits. The basement rocks exposed at Gabal Gerf and Wadi Hodein areas in the southern part of the Eastern Desert of Egypt are represented by sequence of allochthonous ophiolitic rock assemblages thrusted over calc-alkaline metavolcanics. These rocks are intruded by syn-to late-tectonic mafic and granitic intrusions. They are nonconformably overlain by Cretaceous sandstone. Both Precambrian and Cretaceous rocks are extruded by Tertiary basalts. The processed digital data of Landsat ETM ratio images and Egyptsat-1 fused band ratio image covering the study areas have been applied. The digital number values (pixel values) and the spectral curves have been delineated for the different encountered basement rocks on both row ETM and false colour composite (FCC) ratio images. This study revealed that the Landsat ETM-Egyptsat-1 fused band ratio image (7/4, 3/7, 4/5) can be successfully be applied to discriminate the different varieties of volcanic and granitic rocks at the extreme northern part of the Eastern Desert of Egypt. On the other hand, this study revealed that, the different basement rocks exposed at Gabal Gerf area in the southern part of the Eastern Desert can be accurately discriminated using the false colour composite ratio image (FCC) (5/7, 5/1, 4) in (RGB).

1. INTRODUCTION

The basement rocks of the Eastern Desert of Egypt and south Sinai constitute a part of the Arabian-Nubian Shield (about 100,000 km^2) that has been cratonized around the end of the Precambrian. At the north Eastern Desert of Egypt the basement rocks are largely composed of granites together with lesser outcrops of high-grade gneiss, Dokhan volcanics, and Hammamat sediments or their equivalents. The ophiolitic mélange is highly reduced comparing with the central and south Eastern Desert of Egypt. The basement rocks of the northern Eastern Desert of Egypt was previously described and investigated by many authors (e.g; El Ramly and Akaad, 1960; Schurmann, 1966; El Shazly, 1966; Ghanem, 1972; Dardir, 1973; Akaad and Noweir, 1978 and 1980; Dardir et al., 1982; Shalaby, 1985; El Sheshtawi et al., 1987; Abdel Rahman and Doig, 1987; El Gaby et al., 1990 and Takla et al., 1991a and the Egyptian Mineral Resources Authority (EMRA), 2005). The main objective of this study is to demonstrate the value of variably processed different remotely sensed data in discrimination and mapping the Precambrian rocks in the Eastern Desert of Egypt. This study includes two areas namely; Gabal Gharib area representing the most northern Late Proterozoic Arabian-Nubian Shield segment in Egypt and Gabal Gerf in the extreme south eastern Desert of Egypt is selected representing the Northern Eastern Desert of Egypt.

2. MATERIALS AND METODOLOGY

2.1. Digital image processing

Both study areas are covered by Landsat scenes acquired on July and August, 2003. Gabal Gharib area is covered by 145 km of Egyptsat-1 data acquired on 22 Jun 2009. Both Landsat ETM+ and Egyptsat-1 data were subjected to pre-processing steps including georeferenced to UTM Zone 36 North projection with WGS-84 datum. They were radiometrically enhanced to insure radiometric balance between individual scenes before being mosaiced and

clipped to the study area. The digital image processing techniques have been applied to enhance the data of both Egyptsat-1 and Landsat ETM+.

The digital image processing techniques which have been done can be summarized as follows:

1. Achievement of geometric correction and radiometric balancing then mosaicing of Landsat ETM+ and Egyptsat-1 scenes.

2. Applying High Pass Filter (HPF) transform fusion technique has been done in order to merge the panchromatic Egyptsat-1and Landsat ETM+ images and to enhance the spatial resolution of Landsat ETM+.

3. Investigation of spectral reflectance characteristics of the enhanced Landsat ETM+ bands to select the appropriate bands for the ratio images.

4. Applying the band ratio techniques to improve discrimination of the exposed rock units in the study area.

5. Interpretation of the processed images in order to produce the geological map.

2.2. Band-ratio enhancement of remotely sensed data

Band ratio technique is one of the spectral enhancement techniques, which enhance images by transforming the values of each correcting data (Lillesand and Kiefer, 1999). The image processing band-ratio technique is applied by dividing the Digital Number (DN) values of one band by the corresponding DN values of another band and displaying the new DN values as grayscale image (Sabins, 1997). The band-ratio technique has been applied on both Landsat ETM+ and the Egyptsat-1-Landsat fused image in order to enhance the lithological discrimination of the basement rocks encountered in the study areas. Band-ratio technique of both Landsat and Landsat ETM-Egyptsat-1 fused images has been used to enhance spectral discrimination of the exposed basement rocks exposed in Gabal Gharib area. Spectral reflectance curves of different proposed enhanced Landsat band-ratios were tested including; (5/1, 7/4, 3/7), (4/5, 3, 7/1), 7/3, 7/1, 2/3), (7/4, 3/7, 4/5) and the false colour composite ratio image (5/7, 5/1, 4) covering Gabal Gerf area in RGB.

2.3. Landsat ETM+ Egyptsat-1data fusion

Egyptsat-1 is the first spacecraft in the Egyptsat series; it is an earth observation satellite which was successfully put in orbit on 17/04/2007. The data of Egyptsat-1 can be used in a variety of applications in the fields of cartography and photogrammetry. It carries three sensors, multispectral (MS), panchromatic (PAN) and middle infrared (MIR) providing data with spatial resolution of 7.8 m for both MS and PAN and 39 m for the NIR. Egyptsat-1 will open up the usage of the satellite data in Egypt indifferent applications such as thematic mapping of earth surface, urban and disaster management support. It is expected to serve as the vital information source to the remote sensing and GIS community. (Table 1) shows the characteristics of both Egyptsat-1 and Landsat ETM.

Data integration is applied to the remote sensing data with various techniques (Bretschneider and Kao, 2000). In the present study High Pass Filter (HPF) transform data fusion technique was applied whereas Egyptsat-1 panchromatic image data covering Gabal Gharib area was fused with Landsat ETM+ using this technique. The HPF resolutionmerge function allows combination of high-spatial resolution panchromatic data with lower spatial resolution multispectral data to produce new fused image with both excellent detail and a realistic representation of original multispectral scene colours. Landsat ETM-Egyptsat-1fused image preserves a perfect spatial resolution (7.8 m) and the best spectral discrimination (7 spectral bands) of the exposed basement rock units in the study area due to the advantage of the multispectral bands of the Landsat ETM+ data. As well as fractures and joints can be shown very clear in the central part of Gabal Gharib granitic intrusion due to the effect of merge function (Fig. 1).

3. GEOLOGICAL SETTING

3.1. Gabal Gharib area

Gabal Gharib area covers about 580 km2 between Latitudes 27° 59′ 53″ and 28° 10′ 50″ N and Longitudes 32° 39′ 21″ and 32° 57′ 17″ E , with distance about 30 km west of Ras Gharib town on the Gulf of Suez coast. of Landsat ETM-Egyptsat-1 fused images with field checks for discrimination of the exposed basement rocks at Gabal Gharib

area and modifying the published geological maps for this area. The northern part of the Eastern Desert of Egypt which in turn constitutes a part of the larger Pan-African Orogeny. The Late Proterozoic Precambrian basement rocks forming Gabal Gharib area are composed essentially of calc-alkaline metavolcanics, syn to late tectonic mafic and granitic intrusions (G1 and G2), Dokhan volcanics, and post tectonic-alkaline riebeckite granitic intrusions (G3). These rocks are dissected by various dykes and veins. On the other hand, they are unconformably overlain by Neogene and Quaternary deposits. The mapped basement rocks are discriminated on the Landsat ETM-Egyptsat fused band ratio image (7/4, 3/7, 4/5) in (RGB). The discrimination is based on the spectral characterizations which reflect the characteristic colours on the applied fused band ratio image previous mapping and field checks.

3.2. Gabal Gerf Area

Gabal Gerf area is made up mainly of a sequence of metamorphic and magmatic assemblages. The metamorphicassemblage comprises ophiolitic serpentinite-talc carbonate rocks with basic metavolcanics pillowed in parts. They arestructurally thrusted over the metasediments and calc-alkaline schistose metavolcanics. This sequence is intruded byrocks of the magmatic assemblage including syn-late tectonic gabbro-diorite, tonalite, late tectonic layered gabbro and monzogranite intrusions as well as dykes and veins.

Table 1: The main characteristics of Egyptsat-1 and Landsat ETM+ image data covering Gabal Gharib area

Characteristics	**Optical Imaging Systems**			
	Egyptsat-1		**Landsat ETM+**	
Nationality	Egypt		United Stat of America	
Launch date	April 17, 2007		April 15, 1999	
Acquisition date	Jun 2009		July and August 2003	
Swath width	46 km (MSS) 55 Km (MIR)		185 km	
Altitude	668 km		750 km	
Spectral resolution (number of bands and band width)	VNIR	b1 = (0.51 – 0.59 µm) b2 =(0.61 – 0.68 µm) b3 =(0.80 – 0.89 µm)	VNIR	b1= (0.45-0.515 µm) b2= (0.525-0.605 µm) b3= (0.63-0.690 µm) Panchromatic= (0.52-0.90 µm)
	Infrared	(1.1 – 1.7 µm)	Infrared	b4= (0.75- 0.90 µm) b5= (1.55-1.75 µm) b7= (2.09-2.35 µm)
			Thermal I R	b6= (10.40-12.5 µm)
Spatial resolution	VNIR bands: 7.8m- Mid Infrared band: 46 m		Visible-Mid infrared bands 1, 2, 3, 4, 5, 7= 30 m	
	Panchromatic band: 7.8 m		Panchromatic band = 15 m	
			Thermal bands = 60 m	

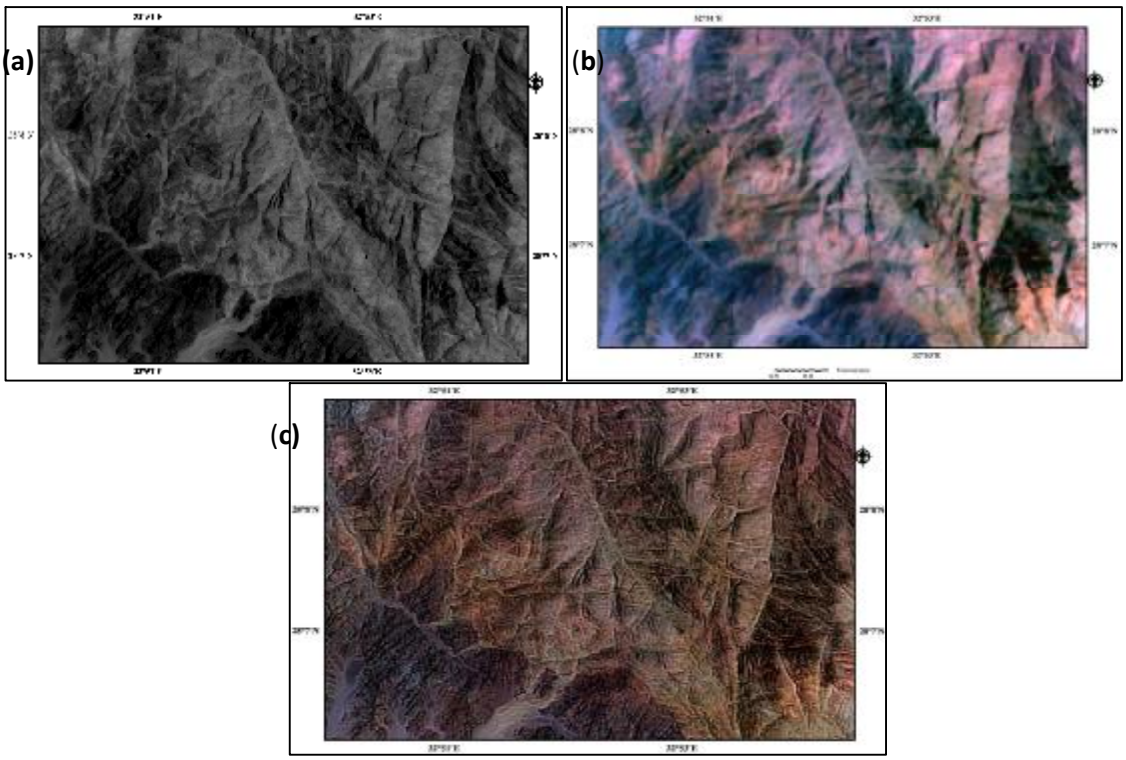

(Figure 1): The central part of Gabal Gharib granitic intrusion. **(a)** Panchromatic Egyptsat-1 image (with 7.8 m spatial resolution). **(b)** False colour composite image 2, 4, 7 on RGB of raw Landsat ETM+ imag (with 30 m spatial resolution). **(c)** Landsat ETM- Egyptsat-1fused image.

3. SPECTRAL CHARACTERIZATION

The ETM data can be used with reliability to distinguish serpentinite from the surrounding rocks in arid regions and to generate detailed maps over wide regions. Composites of the visible bands displayed in red, green and blue show a certain degree of lithological differentiation of the high strain metamorphics and the diagnostic curvilinear tectonics (flow lineaments) which bound these schistose rocks. Similar processing on the ETM image bands 7, 4, 2 gave improved lithological discrimination particularly within the schistose rocks and massive intrusions. Sub-parallel dyke swarms in the granitic plutons can readily be distinguished.Hybrid colour ratio composites were then produced for selected scene. Spectral band ratioing on a pixel by pixel basis tends to enhance minor spectral variations of materials and also minimizes the effects of brightness variations due to topographic aspects. This type of imagery then becomes interpretable in terms of the spectral properties of rocks and minerals and is superbly illustrated by a colour ratio. The mid wave infra red spectral range of TM bands 5 and 7 allow detection of clays, carbonates and hydroxyl-bearing silicate materials present in metamorphosed volcanics and ultramafic rocks. The band ratios 5/7 and 5/1 were selected to enhance the absorption features caused by OH- ion in clays and silicate minerals and the Fe-O charge transfer effect in limonite respectively. Band 4 is being used to provide the morphological informations lacking in the ratios. These ratios were displayed (to red and green) together with band 4 (to blue) to form the hybrid colour ratio composite.

This approach is similar used by other workers (e.g. Yousif and Shedid, 1999; Sultan, 1987) for mapping serpentinite at the Barramiya and Meatiq dome areas respectively; Hassan, 2003; Sadek, 2004 and 2005 and Sadek et al, 2006) Sadek (2004) used the false colour composite landsat ratio images to discriminate the basement rocks exposed at the southern Eastern Desert including Shalatein area (north of the study area) where the ophiolitic assemblage (serpentinite) is less abundant while the calc-alkaline metavolcanics are most predominant. Superficial and residual wadi deposits especially those developed on the late and post tectonic granites are displayed as blue tone due to their high response in band 4. In contrast, basic-intermediate volcanics and the late tectonic gabbroic intrusion (Gabal Korabkansi) produce low 5/1 ratios and tend to show up as a complex colour pattern of dull and very dark green. These rocks are detected on the false colour composite image by an orange-red tone which is symptomatic of the presence of altered olivine and other hydroxyl minerals. The metasediments are conspicuous on the ratioed imagery by a very dark tone indicating relatively strong absorption in both near infra red and visible bands. Training sets representing the eight main lithologic units have been selected to extract the pixel digital number values (DNs) of their spectral reflectances on both the raw image and the FCC ratio image (5/7, 5/1, 4).

They include ophiolitic serpentinite (Gabal Gerf), basic metavolcanics (Gabal Hadal Darjah), calc-alkaline intermediate-basic metavolcanics (north Gabal Madara), syn-tectonic gabbro (east Gabal Gerf), late tectonic layered gabbro (the southern part of Gabal Korabkansi), syn-tectonic tonalite-granodiorite (east Gabal Korbiai) and late tectonic monzogranite (west Gabal Abu Hadid). Pixel digital numbers of the selected points in different bands and band ratios were automatically calculated by ERDAS IMAGINE software 8.7 and listed in (Tabl 3).

Applying the Landsat raw image data, the spectral signature curves of the examined basement rocks show almost the same trends (Fig. 2). The different varieties of the same lithologic unit can not be easily discriminated (e.g. the varieties of metavolcanics, gabbroic and granitic rocks). On the other hand, the spectral signature curves of these examined basement rocks applying the data of false colour composite (FCC) ratio image (5/7, 5/1, 4) show variable. They are discriminated at band ratio 5/1. Accordingly, on this image the serpentinite-talc carbonate rocks exhibit red tone and the metasediments show light green colour. The ophiolitic metavolcanics (yellowish-reddish green) can be discriminated from the calc-alkaline metavolcanics (dark green), the syn-tectonic tonalite-granodiorite (green to dark green) are discriminated from the late tectonic monzogranite (bluish green) and the syn-tectonic gabbro (green-dark green) can be discriminated from the late tectonic layered gabbro(yellowish green).

4. RESULTS AND DISCUSSIONS

Almost all the exposed basement rocks in the northern Gabal Gharib area area have high reflectance at both Landsat ETM+ bands 3 and 5 at wavelength region (0.63-0.690 and 1.55-1.75 µm) respectively, while all these rocks show low reflectance at wavelength regions (0.525-0.605, 0.75-0.90 and 2.09-2.35µm) corresponding to Landsat ETM+ bands 2, 4 and 7 respectively (Table 2). The average spectral reflectance curves of each of the exposed rock units were subsequently compared.

At band 5 both Dokhan volcanics and gabbro-diorite rocks exhibit the same DN values (76), while at band 4 Dokhan volcanics shows higher DN (71) than gabbro-diorite (64). Inspite of at band 7 Dokhan volcanics exhibit lower DN (66) than gabbro-diorite (69). So 7/4 band ratio can discriminate between these two rock units. At Landsat ETM band 4 (0.75-0.90 µm), both monzogranites and reibeckite granites exhibit the same DN values. At bands 3 and 7 riebeckite granites show the same DN values, while monzogranites have different DN values 114 and 96 respectively, therefore, monzogranites and the post tectonic riebeckite granites can be discriminated by the band ratio (3/7).

At bands 4 and 5, the calc-alkaline metavolcanics show the same DN values while the alkali feldspar granites show different DN values 84 and 111 respectively. So the band ratio (4/5) can discriminates between these two rock units. Data integration is applied on Egyptsat-1 and Landsat data using High Pass Filter fusion (HPF) technique in order to get more enhanced remotely sensed data. Landsat ETM+ Egyptsat-1 fused image preserves a perfect spatial resolution (7.8 m) and the best spectral discrimination (7 spectral bands) of the exposed rock units in the study area due to the advantage of the multispectral bands of the Landsat ETM+ data (Fig. 2). Applying the Landsat ETM raw data, the spectral curves are nearly parallel and the rock units are poorly discriminated (Fig. 3a), while these rocks show much better discrimination applying the data of the ETM-Egyptsat-1 fused band ratio image (7/4, 3/7, 4/5) in (RGB) (Fig. 3b). The modified geological map is produced based on the previous mapping, interpretation of the Landsat ETM+ Egyptsat-1 fused image, spectral characterizations of the different rock units and field checks (Fig. 4). At Gabal Gerf area, this study revealed that the ETM image bands 7, 4, 2 improve the lithologic discrimination of the schistose rocks and massive granitic intrusions and distinguish the linear features such as faults and dyke swarms. On the other hand the different basement rock assemblages as well as the different varieties of the same lithologic unit exposed in the Gabal Gerf area can be accurately discriminated using the false colour composite (FCC) ratio ETM image 5/7, 5/1, 4 (RGB)(Fig. 5). Applying the Landsat raw image data, the spectral signature curves of the examined basement rocks show almost the same trends (Fig. 6, A). The different varieties of the same lithologic unit can not be easily discriminated (e.g. the varieties of metavolcanics, gabbroic and granitic rocks (Fig. 6,B). On the other hand, the spectral signature curves of these examined basement rocks applying the data of false colourcomposite (FCC) ratio image (5/7, 5/1, 4) show variable trends (Fig. 14). They are discriminated at band ratio 5/1.Accordingly, on this image the serpentinite-talc carbonate rocks exhibit red tone and the metasediments show light greencolour. The ophiolitic metavolcanics (yellowish-reddish green) can be discriminated from the calc-alkaline metavolcanics (dark green), the syn-tectonic tonalite-granodiorite (green to dark green) are discriminated from the late tectonic monzogranite (bluish green) and the syn-tectonic gabbro (green-dark green) can be discriminated from the late tectonic layered gabbro (yellowish green. Finally modified geological map is produced with more details than the published geological maps for Gabal Gerf area (Fig. 7).

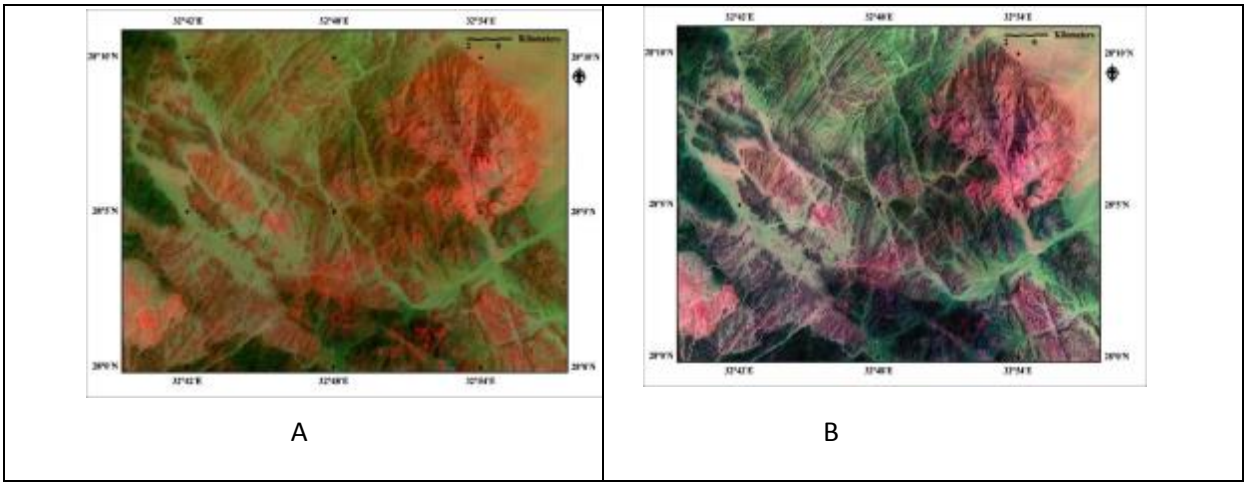

(Figure 2): Landsat ETM+ band ratio image (7/4, 3/7, 4/5) assigned in (RGB (A) Landsat ETM- Egyptsat-1 fused band ratio image (7/4, 3/7, 4/5) assigned in (RGB (B).

Table 2: Average DN values for the exposed rock units in various spectral bands of Landsat ETM+ covering Gabal Gharib area

Rock unit/ Spectral band	**DN values**					
	1	**2**	**3**	**4**	**5**	**7**
Calc-alkaline metavolcanics (va)	84	76	89	64	64	56
Gabbro-diorite (dr)	85	77	90	64	76	69
Tonalite-granodiorite (gd)	90	84	102	74	90	83
Dokhan volcanics (dv)	87	81	97	71	76	66
Monzogranite (gm)	94	91	114	85	103	96
Alkali feldspar granite (gk)	90	88	109	84	111	103
Alkaline riebeckite granites (gr)	89	87	106	84	109	106

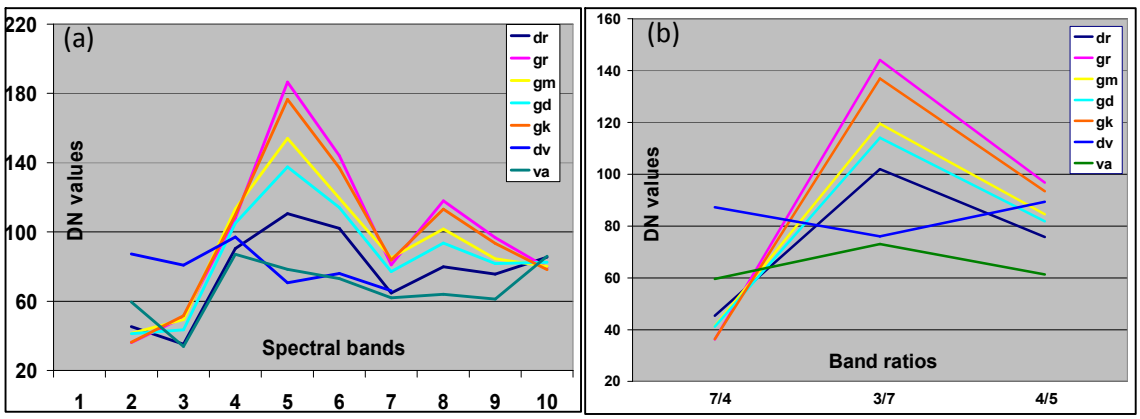

Figure 3: **(a)** Spectral characteristic curves showing poorly discrimination for the exposed basement rocks in Gabal Gharib area with applying the Landsat ETM+ raw data**. (b)** Spectral characteristic curves showing better discrimination for the exposed basement rocks with applying the data of Landsat ETM-Egyptsat-1 fused band ratio image (7/4, 3/7, 4/5) showing more accurate lithological discrimination.

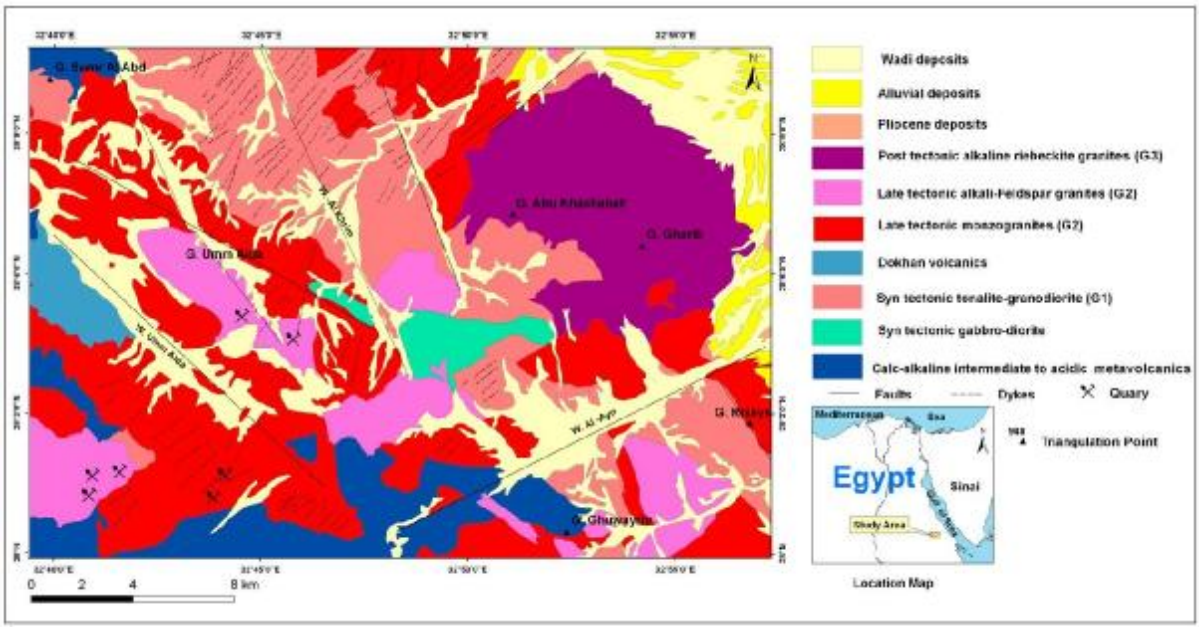

(Figure. 4): Geological map of Gabal Gharib area modified after Egyptian Mineral Resources Authority (2005).

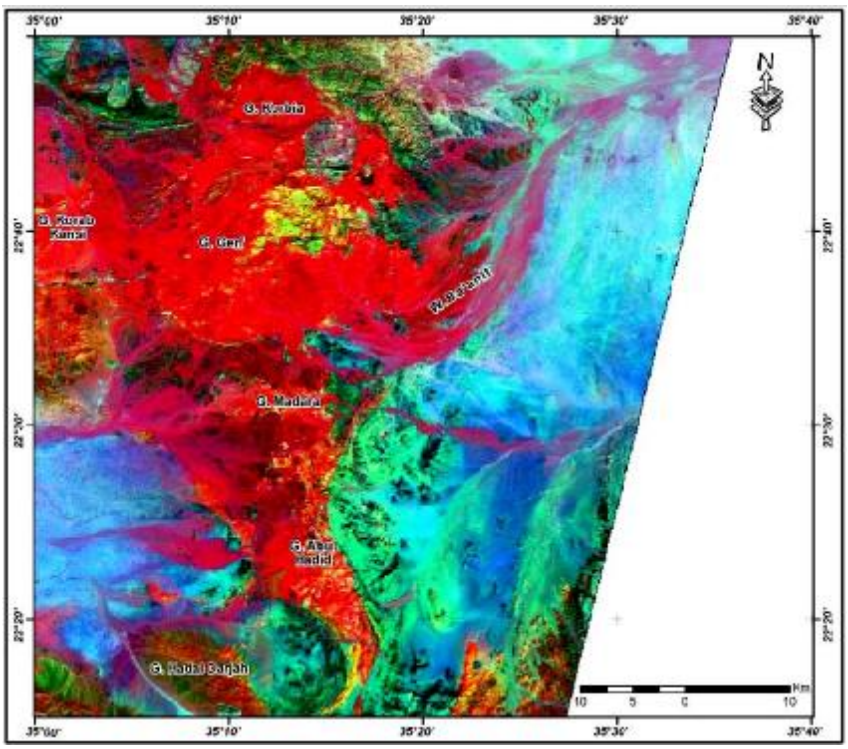

(**Figure 5):** False colour composite (FCC) ratio ETM image (5/1, 5/7, 4) of the study Gabal Gerf area.

(Table 3): Average DN values for the exposed rock units in various spectral bands of Landsat ETM+ covering Gabal Gerf area.

Rock units/ spectral Band	**DN values**								
	1	**2**	**3**	**4**	**5**	**6**	**7**	**5/7***	**5/1***
Ophiolitic Serpentinite	51	43	50	38	42	33	46	119	84
Ophiolitic MV	56	50	56	46	67	57	53	117	79
Metasediments	78	71	96	74	102	91	84	104	129
Calc-alkaline MV	54	46	52	39	45	38	48	106	77
Syntectonic Gabbro	71	64	73	49	72	64	58	106	105
Tonalite-granodiorite	74	68	88	63	96	83	66	115	138
late tectonic gabbro	55	49	54	43	60	50	49	112	60
Late tectonic monzogranite	88	89	111	81	110	96	85	107	120

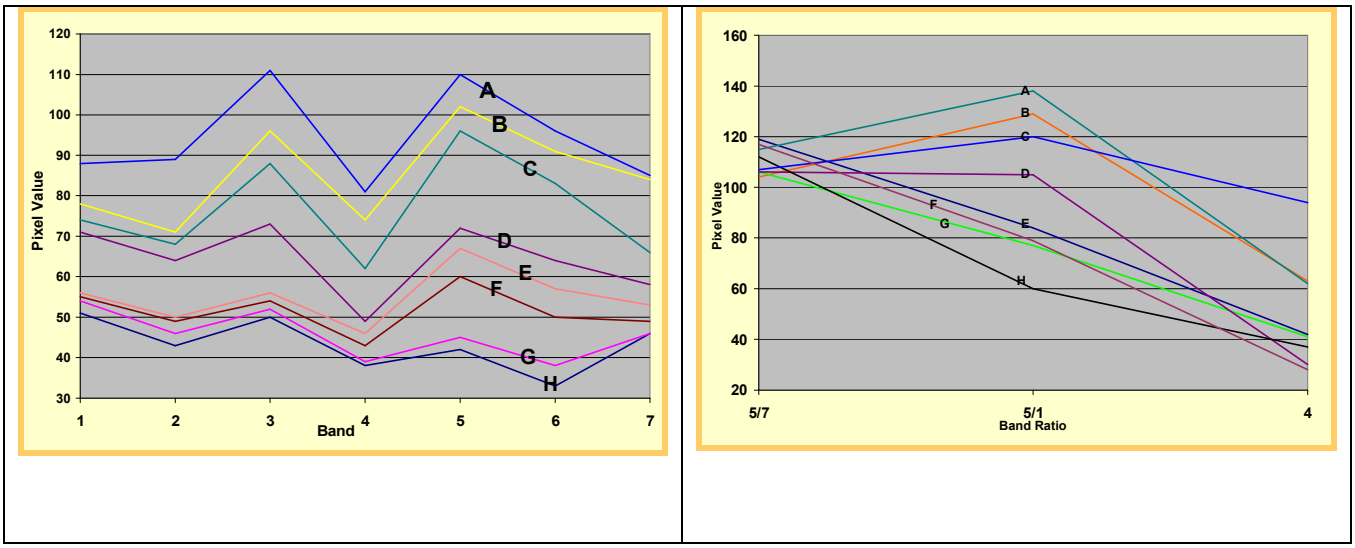

a **b**

(Figure 6): (a) Spectral characteristic curves showing poorly discrimination for the exposed basement rock units with applying the Landsat ETM+ raw data. (b) Spectral characteristic curves showing better discrimination for the exposed basement rock units with applying the data of Landsat ETM-Egyptsat-1 fused band ratio image (7/4, 3/7, 4/5) showing more accurate discrimination of the different rock units exposed at Gabal Gharib area.

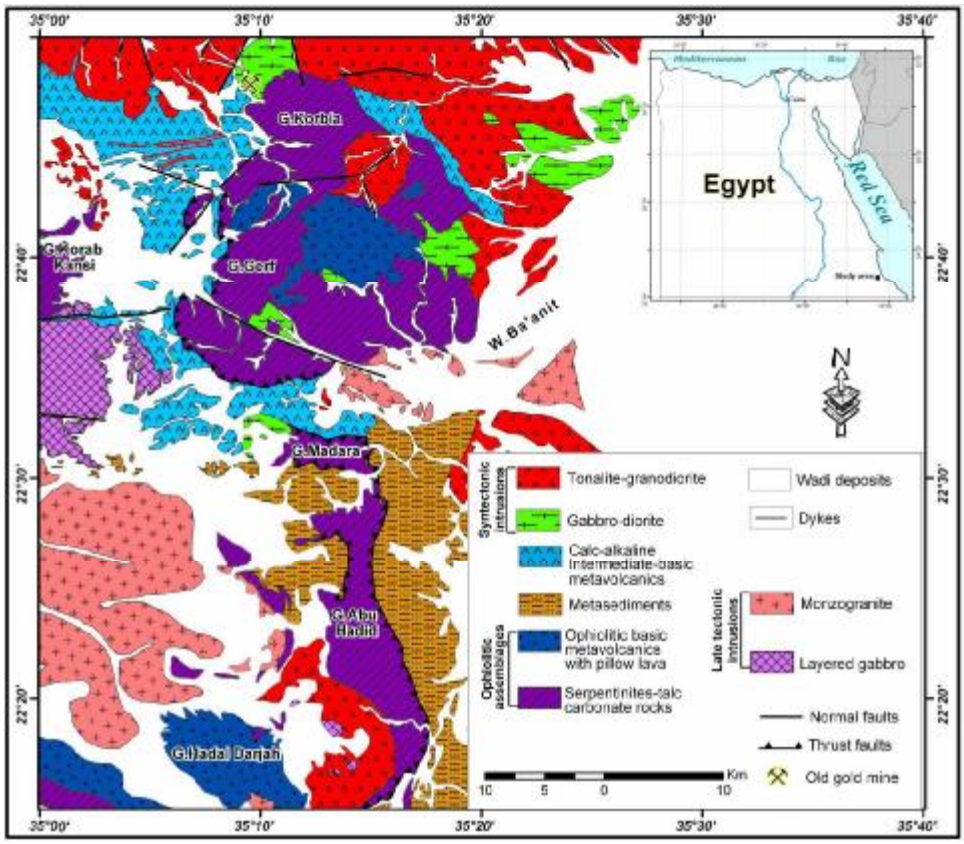

(Figure 7): Geological map of Gabal Gerf area, produced from the data interpretations of field study and FCC band ratio image (5/1, 5/7, 4) and the previous mapping..

REFERENCES

Abdel Rahman, A. M. and Doig, R., 1987. The Rb/Sr geochronological evolution of the Ras Gnarib segment of the northern Nubian Shield. J. Geol. Soc. London., V. 144, pp. 577-586.

Akaad, M. K., and Noweir, A. M., 1978. Geology and lithostratigraphy of the Arabian Desert orogenic belt of Egypt between latitudes 25° 35' and 26° 30' N. In "Evolution and Mineralization of the Arabian-Nubian Shield Symposium IAG Jaddah, Abstract Precambrian Research, 6, A 6.

Akaad, M. K., and Noweir, A. M., 1980. Geology and lithostratigraphy of the Arabian Desert orogenic belt of Egypt Geol. Jaddah, Bull. 4, V. 3, PP. 127-134.

Bretschneider, T. and Kao, O., 2000. Image fusion in remote sensing. Proceedings of the first Online Symposium of Electronic Engineers. CD-Rom.

Dardir, A. A., 1973. Geology of the northern part of Arabo-Nubian Shield. Novieusledovaniya Geologia, No. 5, Leningrad.

Dardir, A.A., Awadallah, M.F. and Abu Zid, K.M., 1982. A new contribution to the geology of Gabel Dokhan, Eastern Desert, Egypt. Ann. Geo. Surv. Egypt, V. 12, 19-27.

Egyptian Mineral Resources Authority, 2005. Geological map of Jabal Gharib area, Egypt, Scale, 1:100,000.

El Gaby, S., 1975. Petrochemistry and geochemistry of some granites from Egypt N. Jb. Miner Alt.V.124, pp. 147-199.

El Gaby, S., List, F. K. and Tehrani, R., 1990. The basement complex of the Eastern Desert and Sinai. Said R. (ed.), The geology of Egypt. Bolkema-Rotterdam-Brookfield, pp. 175-184.

El Ramly, M, F. and Akaad, M. K., I960. The basement complex in the Eastern Desert of Egypt between latitudes 24° 30' and 25° 40' . Geol. Surv. Egypt, paper No. 8.

El Shazly, E. M., 1966. Structural development of Egypt. 4th Anna Meet., Geol. Soc. Egypt, Cairo, pp. 31-38.

El- Sheshtawi, Y.A., Ali, M.M., Salman, A.B. and Hammoda, E.A. , 1987. Textural patterns, geochemistry and origin of the granitoid rocks in the north Eastern Desert of Egypt. Bull. Fac. Sci. Zagazig Univ. V. 9, pp. 256-299.

ERDAS, 1999. "Earth Resources Data Analysis System, ERDAS Field Guide", Fourth Edition, ERDAS Inc., Allanta, GA., USA.

Ghanem, M., 1972. Geology of the basement rocks north of latitude 28° 00' N, Eastern Desert, Ras Gharib area. Ann. Geol. Surv. Egypt., V. 2. pp. 181-198.

Hassan, S.M., 2003. Geoenvironmental study in Shalatein area, South Eastern Desert of Egypt using remote sensing and GIS techniques. Msc. Thesis. Institute of Environmental Studies and Research, Ain Shams University, Cairo, Egypt.

Lillesand, T. M. and Kiefer, R. W., 1999. Remote Sensing and image interpretation. Thomas M. Lillesand, Ralph W. Kie Fer. Fourth edition Ressetar. R. and Monrad, J. R., 1983. Chemical composition and tectonic setting of the Dokhan volcanic Formation, Eastern Desert, Egypt. J. African Earth Sciences, V. 1, No. 2, PP. 103-112.

Sabins, F., 1997. Remote Sensing Principles and Interpretations. W.H. Freeham and Co., New York.

Sadek, M.F., 2004. Discrimination of basement rocks and alteration zones in Shalatein area, southeast Egypt using Landsat TM Imagery Data. Egypt. J. Remote Sensing and Space Sci., V. 7, pp. 89-98.

Sadek, M.F., 2005. Geology and spectral characterization of the basement rocks at Gabal Gerf area, Southeastern Egypt. Egypt. J. Remote Sensing and Space Sci., V. 8, pp.109-128.

Sadek, M.F., Ramadan, T.M., Abu El Leil, I. and Salem, S.M., 2006. Using remote sensing techniques in lithological discrimination and detection of gold-bearing alteration zones at Wadi Defeit area, southeastern Egypt. Proc. of SPIE Vol. 6366-18. Remote Sensing for Environmental Monitoring GIS Applications and Geology VI, 13-14 September, 2006, Stockholm, Sweeden.

Schurmann, H. M. E., 1966. The Precambrian along the Gulf of Suez and northern part of the Red Sea. E. J. Brill, Leiden, the J. Remote Sensing and Space Sci., V. 7, pp, 89-92, Netherlands, 404 p.

Shalaby, M. H., 1985. Geology and radioactivity of Wadi Dara area, northern Eastern Desert, A. R. E. Ph.D. Thesis, Faculty of Science, Alexandria University, Alexandria, Egypt, 165p.

Sultan, M.; Arvidson, R.E.; Sturchio, N.C. and Guinness, E.A., 1987. Lithologic mapping in arid region with Landsat Thematic Mapper data. Meatiq Dome, Egypt. Geol. Soc. Amer. Bull., 99, 748-762.

Takla. M. A., Khalaf, I. M., All, M. M. and Eliwa, H. A., 1991a. The granitoide of Gabal Umm Tenassib, northern Eastern Desert, Egypt. Egyptian Miner., V. 3, pp. 95-117.

Yousif, M.S. and Shedid, G.M., 1999. Remote sensing signature of some selected basement rock units from the Central Eastern Desert of Egypt. Egypt. J. Remote Sensing and Space Sci., V. 2, pp. 1-14.